

# Two Flagellar Genes, *AGG2* and *AGG3*, Mediate Orientation to Light in *Chlamydomonas*

Carlo Iomini,<sup>1,2,\*</sup> Linya Li,<sup>2</sup> Wenjun Mo,<sup>3</sup> Susan K. Dutcher,<sup>2,\*</sup> and Gianni Piperno<sup>1</sup>

<sup>1</sup>Department of Molecular, Cellular, and Developmental Biology

Mount Sinai School of Medicine  
1 Gustave L. Levy Place  
Box 1007

New York, New York 10029

<sup>2</sup>Department of Genetics  
Washington University School of Medicine  
660 South Euclid Avenue  
St. Louis, Missouri 63110

<sup>3</sup>Biogen Idec  
12 Cambridge Center  
Cambridge, Massachusetts 02142

## Summary

Ciliary membranes have a large repertoire of receptors and ion channels that act to transduce information from the environment to the cell. *Chlamydomonas* offers a tractable system for dissecting the transport and function of ciliary and flagellar membrane proteins. Isolation of ergosterol and sphingolipid-enriched *Chlamydomonas* flagellar membrane domains identified potential signaling molecules by mass spectroscopy. These include a membrane protein and a matrix flavodoxin protein that are encoded by the *AGG2* and *AGG3* genes, respectively. Agg2p localizes to the proximal flagellar membrane near the basal bodies. Agg3p is distributed throughout the flagellar matrix, with an increased concentration in the proximal regions where Agg2p is located. *Chlamydomonas* cells sense light by using a microbial-type rhodopsin [1], transduce a signal from the cell body to the flagella, and alter the waveform of the flagella to turn a cell toward the light. Protein depletion by RNA interference reveals that both *AGG* gene products play roles in the orientation of cells to a directional light source. The depleted strains mimic the phenotype of the previously identified *agg1* mutant, which swims away from light. We propose that the localization of Agg2p and Agg3p to the proximal region of the flagella may be important for interpreting light signals.

## Results and Discussion

### Characterization of Flagellar DRM Proteins

Ciliary defects are associated with polycystic kidney disease, situs inversus, retinal degeneration, Bardet Biedl Syndrome, and Hedgehog signaling defects. Autosomal dominant polycystic kidney disease results primarily from mutations in two membrane proteins,

polycystin-1 and polycystin-2, that localize to cilia as well as to the endoplasmic reticulum (reviewed in [2]). *Chlamydomonas* flagella generate and receive sensory signals in addition to their role in motility. These signals include partner recognition during mating (reviewed in [3]) and responses to changes in the intensity and direction of light.

To identify proteins that potentially mediate signaling, we purified detergent-resistant membranes (DRMs) from isolated *Chlamydomonas* flagella membranes (see [Supplemental Experimental Procedures](#) available with this article online; [Figure 1E](#)). DRMs are membrane fragments that are enriched in sterols and sphingolipids but deprived of unsaturated glycerophospholipids [4]. In sucrose gradients, isolated DRM proteins formed a peak of concentration between fractions 9 and 13, and the proteins were then resolved as four electrophoretic bands indicated by the numbers in [Figure 1A](#). The radioactivity from <sup>35</sup>S-labeled proteins associated with DRMs represents 5% and 0.4% of membrane and flagellar radioactivity, respectively (data not shown). This preparation has a simpler composition than DRMs isolated from yeast membranes [5]. DRM preparations are expected to be rich in ergosterol and sphingolipids. This premise was tested with nystatin, a sterol binding compound that displaces proteins from detergent-resistant membranes [4]. Nystatin treatment of isolated flagella at concentrations of 0.2 or 0.7 units/μl extracts 40% and 70% of the proteins from DRM-enriched fractions, respectively. Sphingolipids were resolved by chromatography on thin-layer silica gels (data not shown). <sup>35</sup>S-labeled sphingolipids were 3.5 times more concentrated in DRMs than in the membrane fraction (see [Supplemental Experimental Procedures](#)).

To identify the proteins, we digested each band with trypsin to generate peptides for analysis by mass spectrometry ([Figure 1A](#)). Bands 1 and 3 both yielded a single peptide of 11 amino acids. This peptide identifies a hypothetical protein of 19,570 D (protein name at DOE/JGI: 152872. GenBank accession number for the mRNA: DQ065847. Subsequently, these are given in the format protein name/accession number); this protein contains predicted transmembrane domains between amino acids 20 and 42 and between amino acids 49 and 71. Band 2 was analyzed from four independent purifications and yielded three peptides that identify three predicted proteins ([Figure 1A](#)). One peptide identifies a 15,624 D protein (152871/DQ065848). This and the 19,570 D protein from band 1 are likely to be paralogs because they show 63% identity and 68% similarity ([Figure S1](#)). They share a PLAC8 Pfam domain or DUF614 domain that is broadly conserved in eukaryotes but has an unknown function. In two preparations, mass-spectrometry analysis yielded an additional two peptides that both identify predicted proteins of 21,386 D and 21,414 D (155909/DQ408775 and 155892/DQ408776). These two proteins differ by only seven amino acids and both contain a 156 amino acid predicted flavodoxin

\*Correspondence: ciomini@genetics.wustl.edu (C.I.); dutcher@genetics.wustl.edu (S.K.D.)

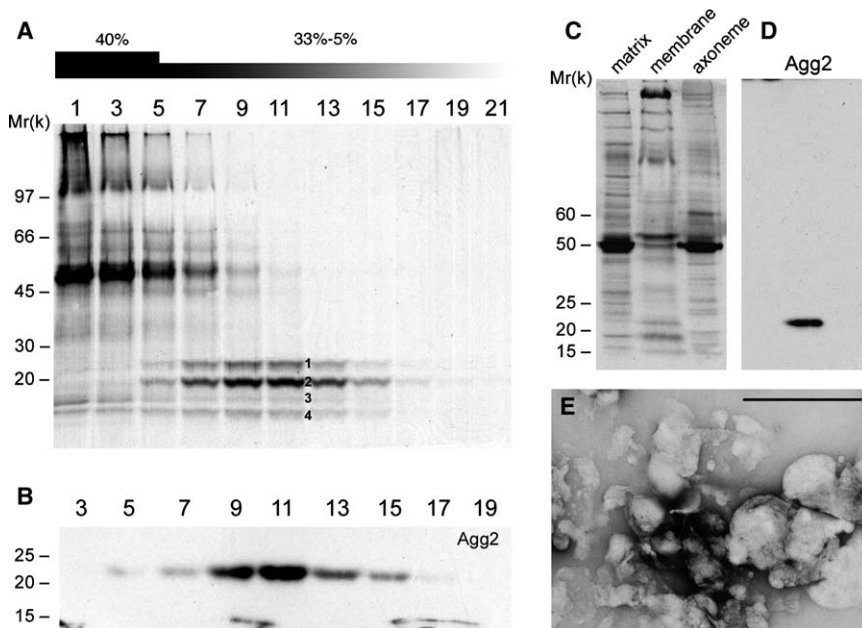


**Figure 1. Agg2p Is a Flagellar Membrane Protein**

For DRM isolation, *Chlamydomonas* flagella were detached from the cell bodies by a change in the pH of the medium and separated from the cell bodies by centrifugation [26]. The membranes were released from the microtubule axoneme by two cycles of freeze-thawing [27], and the membrane, matrix, and axonemes were separated by ultracentrifugation on a discontinuous gradient formed by 10%, 30%, 40%, and 45% layers of sucrose. The 40% sucrose fraction containing membranes (1E) was exposed to 1% Triton-X 100 at 4°C and loaded under a 33%–5% sucrose gradient. DRMs floated upwards and formed a peak of concentration between fractions 9 to 13, whereas the majority of the extracted proteins remained in the 40% sucrose fractions (fractions 1–5).

(A) Autoradiogram of <sup>35</sup>S-labeled polypeptides in sucrose gradient fractions 1–21 resolved by polyacrylamide gel electrophoresis. Numbers between the lanes labeled 11 and 13 indicate bands 1–4. Direction of floatation is from the left. Positions of molecular-weight standards are indicated on the left.

(B) An immunoblot of an electrophoretogram similar to one shown in (A) reacted with the His-Agg2p antibody (polyclonal antibody specific for His-tagged Agg2p).

(C) Autoradiogram of <sup>35</sup>S-labeled polypeptides present in the 10% and 40% sucrose fractions and pellet.

(D) An immunoblot of the electrophoretogram shown in (C) reacted with the his-Agg2p antibody.

(E) Electron microscopy of negatively stained samples revealed that the 40% sucrose fraction had irregular disks or vesicles smaller than 1 μm in diameter. Axonemes were absent from this fraction. The scale bar represents 1 μm.

domain (Figure S2). Band 4 did not yield any peptides. For simplicity, we refer to DQ065847 as AGG2 and to DQ408775 as AGG3. The loci names, AGG2 and AGG3, were chosen based on the below-described functional studies that reveal a phototaxis phenotype similar to that of the *agg1* mutant [6].

### Agg2p Is a Membrane Protein that Localizes to the Proximal Flagellar Region

A polyclonal antibody against bacterially expressed, tagged Agg2p detects Agg2p in the DRM fractions (Figure 1B) and in the membrane fraction (Figures 1C and 1D) but not in flagellar matrix or axonemal fractions (Figures 1C and 1D). In addition, Agg2p is detectable in whole-cell extracts by immunoblots when 5-fold more radioactivity is analyzed (data not shown). Agg2p localizes to the proximal region of flagella that has 9 + 0 microtubules and is likely to extend into the region with 9 + 2 microtubules (Figures 2A, 2B, 2G, 2H, 2I, 2J, 2K, 2L, and 2M). Upon deflagellation, the flagellar-localized Agg2p remains with the isolated flagella and not with the cell body (Figures 2C–2F). When the cell wall is removed by autolysin and the resulting protoplasts are extracted with a nonionic detergent to allow increased internal staining (see Supplemental Experimental

Procedures), Agg2p is detected at two additional sites (Figures 2G–2M, arrowheads) near the distal striated fibers, which contain centrin (Figures 2N–2P arrow). The Agg2p staining does not overlap the location of IFT71, a complex B subunit of the intraflagellar transport machinery that encircles the basal bodies [7, 8] (Figures 2Q–2T).

Other signaling molecules, which include TRP (transient receptor potential) channels (reviewed in [9]) and Smoothed [10], must be localized to the ciliary membrane for their proper signaling activity. Other membrane proteins show nonuniform distributions along cilia or flagella. Polycystin-2 is found in multiple, distinct foci along the primary cilia of granulosa cells in mice [11], at the proximal end of the cilia in *C. elegans*, and at the distal tip of *Drosophila* sperm [12]. Finally, TRPC (transient receptor potential canonical) channels are confined to punctuate patterns along the flagellum of mouse and human sperm and overlap to different extents with components of lipid rafts [13].

Several axonemal proteins have a discrete flagellar localization that could function as anchoring sites for ciliary and flagellar membrane proteins. Nephrocystin-1, which is mutated in type I nephronophthisis, localizes to the proximal region of motile cilia of the respiratory

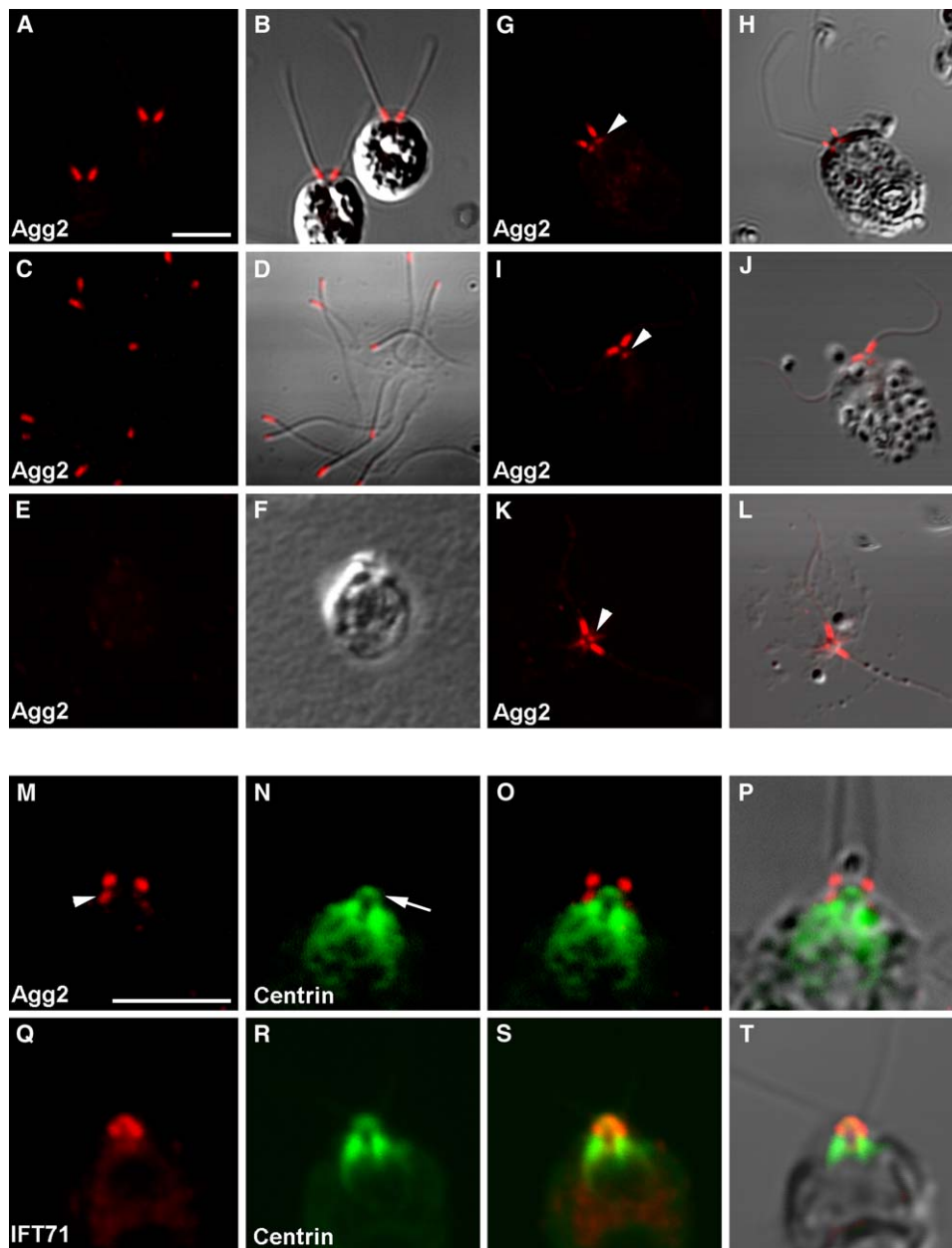


**Figure 2. Agg2p Localizes to the Proximal Region of Flagella and Near the Basal Bodies**

Immunofluorescence signals from His-Agg2p antibody applied to whole cells (A), isolated flagella (C), cell bodies (E), and protoplasts (G, I, K, and M). Arrowheads in (G, I, K, and M) indicate Agg2p basal-body-associated regions of staining. (B, D, F, H, J, and L) Combined immunofluorescence signals from His-Agg2p antibody and differential interference contrast (DIC) micrographs. (N and R) Immunofluorescence signals from a centrin antibody. Arrow in (N) indicates the centrin in the distal striated fibers. (O and S) Merged immunofluorescence signals. (O) His-Agg2p and centrin antibodies. (S) His-IFT71 and centrin antibodies. (P and T) Combined immunofluorescence signals and DIC micrographs. (Q) Immunofluorescence signals from an IFT71 antibody. Scale bars represent 5  $\mu\text{m}$ .

epithelium [14], as do several NIMA-related kinases [15, 16]. To test if Fa2p, a NIMA-related kinase in *Chlamydomonas*, anchors Agg2p, we examined the localization of Agg2p in *fa2-4* cells. Its localization remains indistinguishable between *fa2-4* and wild-type cells (data not shown).

#### **Agg3p Is a Flavodoxin that Localizes to the Flagellar Matrix**

We used a polyclonal antibody against bacterially expressed, tagged Agg3p to examine its localization and

fractionation properties. Agg3p is detected in flagella and in the membrane-plus-matrix fraction but not in the cell body or axonemal fractions (Figures 3A and 3B). When a freeze-thaw method is used, the majority of Agg3p is found in the flagellar matrix fraction, but a small amount is also found in the membrane fraction (Figures 3C and 3D). In these experiments, Agg3p was not detected in the DRM fractions (data not shown). Detectable amounts of Agg3p are observed in cell-body extracts when 5-fold more radioactivity is analyzed by immunoblots (data not shown). By immunofluorescence

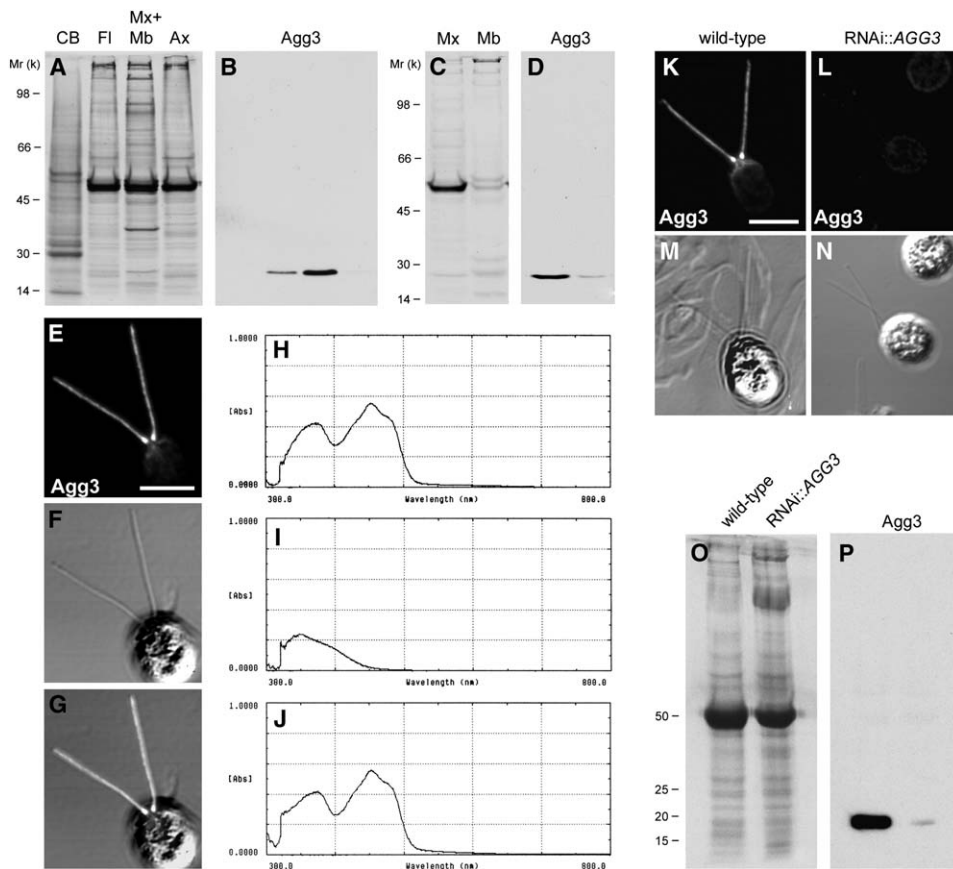


Figure 3. Agg3p is a Flavodoxin Localized to the Flagellar Matrix in Wild-Type 137 mt+ Cells

(A and C) Autoradiograms of  $^{35}\text{S}$ -labeled polypeptides from samples containing equal amounts of radioactivity. (A) Cell bodies, flagella, membrane plus matrix, and axonemes from a wild-type strain. (C) Matrix and membrane fractions from a wild-type strain. (B and D) Immunoblots of (A) and (C), respectively, reacted with the His-Agg3p antibody (polyclonal antibody specific for His-tagged Agg3p). (E) Immunofluorescence signal from the His-Agg3p antibody on wild-type protoplasts. DIC micrograph is shown alone (F) or combined with immunofluorescence signal (G). (H–J) His-Agg3p spectra of absorbance. RNAi::AGG3 transformant has reduced amounts of Agg3p in flagella. (K and L) Immunofluorescence signals from His-Agg3p antibody and (M and N) DIC micrographs of the same microscope field. (O) Autoradiogram of  $^{35}\text{S}$ -labeled polypeptides from flagella of wild-type and RNAi::AGG3 transformant. (P) Immunoblot of the electrophoretogram shown in (O) reacted with the His-Agg3p antibody.

microscopy, Agg3p localizes along the entire length of flagella but concentrates at the proximal region where Agg2p localizes (Figures 3E–3G).

By sequence analysis, Agg3p is a flavodoxin. Flavodoxins are flavin mononucleotide binding redox proteins that act as a hydrogen or electron donor to reduce a hydrogen or electron acceptor. To test this prediction, we analyzed the bacterially expressed His-tagged Agg3 protein by spectroscopy. After purification over a Ni-NTA (NTA, nitriloacetic acid) agarose column, the eluate is yellow and generates an absorbance spectrum that is characteristic of oxidized flavodoxins (Figures 3H–3J) [17]. Upon exposure to  $\beta$ -mercaptoethanol, the absorbance spectrum shifts (Figure 3I). Dialysis of the  $\beta$ -mercaptoethanol and exposure to air reverses the shift, as is observed for other flavodoxins (Figure 3J). Although located in the flagellar matrix, Agg3p may associate weakly with the flagellar membrane. Its concentration at the proximal region of the flagella suggests a possible functional interaction with Agg2p.

### AGG2 and AGG3 Play a Role in Orientation to Light Signals

Using the constitutively expressed tandem inverted repeat construct of Rohr and coworkers [18], we employed stable RNA interference to determine the function of AGG2 and AGG3 (see Supplemental Experimental Procedures). Transformants silence the tryptophan synthetase  $\beta$  gene (*MAA7*) and are selected by growth on medium with 5-fluoroindole (5-FI), a suicide substrate. These colonies are screened by quantitative reverse-transcriptase polymerase chain reaction (RT-PCR) for reductions in the message levels for the gene of interest. Six of the nine 5-FI-resistant transformants showed a 4.2- to 6-fold reduction of the AGG2 mRNA concentration. Two of the four 5-FI-resistant transformants showed a reduction of 5- or 8-fold of AGG3 mRNA. Immunoblots of a RNAi::AGG3 strain (8-fold mRNA reduction) and a RNAi::AGG2 strain (6-fold mRNA reduction) demonstrate that the protein levels were decreased by approximately 80% (Figures 3O and 3P and data not shown). Immunofluorescence of these

A

Genotype	% cells showing positive taxis	% positively tactic that are 5-FI resistant	% negatively tactic that are 5-FI resistant
wild-type (137 mt+)	96 $\pm$ 2.6	NA	NA
<i>agg1</i>	3 $\pm$ 0.5	NA	NA
RNAi::AGG2	25 $\pm$ 1.7	2 $\pm$ 0.5	89 $\pm$ 5.3
RNAi::AGG3	16 $\pm$ 1.5	6 $\pm$ 0.7	92 $\pm$ 4.1

B

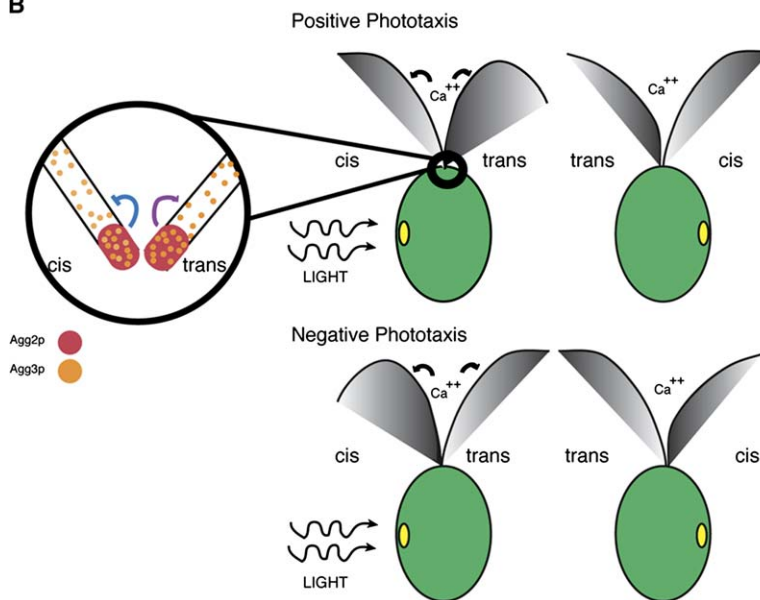


Figure 4. Phototaxis Phenotype and a Schematic Model for a Possible role of Agg2p and Agg3p in Orientation during Phototaxis

(A) Phenotypic analysis of RNAi strains and their RNAi status based on resistance to 5-FI. Each number presented is the average of three independent experiments and the standard deviation.

(B) Positive phototaxis. Light is hitting the eyespot (yellow), and signals are transmitted to the flagellar membrane where calcium channels open. The *trans* flagellum in positive phototaxis is activated as indicated by the larger shaded area under the flagellum. The signals mediated by Agg2p and Agg3p (red and orange dots) may act to inhibit the dynein arms in the *cis* flagellum (purple line) and activate the dynein arms in the *trans* flagellum (blue line). As the cell turns away from the light during its helical swimming path, the signal is lost and the two flagella have more similar waveforms, with lightly larger amplitude for the *cis* flagellum.

(B) Negative phototaxis. The cell shows the reversed response. The *cis* flagellum responds because the inhibition is lost and the *trans* flagellum is not activated.

strains also reveals a dramatic decrease in protein levels (Figures 3K and 3L and data not shown).

Flagella assembly, length, swimming patterns, mating efficiency, meiosis and deflagellation are not affected by depletion of Agg2p or Agg3p (see Supplemental Experimental Procedures). However, all of the RNAi strains show an obvious change in phototactic behavior. These *Chlamydomonas* sense light but respond incorrectly by swimming away from it rather than toward it. Two classes of previously identified mutants move away from light; these are the *mbo* and *agg* mutants. When the light intensity is too high ( $1 \times 10^{22}$  photons/m<sup>2</sup>), the cells use a sinusoidal waveform to back away from the light (photophobic response); the *mbo* mutant cells mimic this behavior under all light conditions [19]. The RNAi strains do not resemble the *Mbo*<sup>-</sup> swimming behavior. The *agg1* mutant uses a breast-stroke waveform but orients away from the light (negative phototaxis) [6]. The RNAi strains behave similarly to the *agg1* strain. To determine if either gene could be the *AGG1* locus, we mapped each with respect to the *IDA5* locus, which is linked to *AGG1* [20]. Mapping data show no linkage (*AGG3:IDA5*, 15 parental to 14 recombinants; *AGG2:IDA5*, 17 parental to 12 recombinants).

The *Agg*<sup>-</sup> phenotype was characterized in liquid cultures with a directional light source. The *AGG2* and *AGG3* strains were compared to wild-type and *agg1* strains. In the RNAi strains, most cells swam away from the light while some cells swam toward the light. Because silencing occurs quickly in these strains upon their removal from selective medium, each population was assayed for growth on 5-FI medium. Approximately 25% of the RNAi::*agg2* cells swam toward the light, but only 2% of these cells were resistant to 5-FI. Among the RNAi::*AGG2* cells that swam away from the light, most showed resistance to 5-FI (Figure 4A). Similar ratios were observed for RNAi::*AGG3* populations (Figure 4A). In all transformants that were grown in the absence of selection, the resistance phenotype and the phototaxis phenotypes were lost within 3–5 weeks. Thus, phenotypes observed in these strains are likely to arise from the reduced levels of RNA and protein rather than the insertional event.

As observed for the naturally occurring variant *agg1*, RNAi transformants with reduced levels of Agg2p or Agg3p swim away from a light source that attracts wild-type cells. The *Agg*<sup>-</sup> pathway(s) must function in wild-type cells to permit positive phototaxis. Because of the helical nature of the swimming, cells receive

alternating periods of light intensity if they are not swimming perpendicularly to a light source. Wild-type *Chlamydomonas* shows positive phototaxis because one of the two flagella responds preferentially to a light signal. Although the two *Chlamydomonas* flagella appear to be similar morphologically, studies on demembrated and reactivated cells show that flagella exhibit a differential response to changes in  $\text{Ca}^{2+}$  concentration [21]. The *cis* flagellum is located in the hemisphere with the eyespot, and the *trans* flagellum is on the other side. In a genetically wild-type strain, the *trans* flagellum is responsive under most physiological conditions. When the eyespot transmits reception of the light signal, the *trans* flagellum responds with a larger amplitude of its waveform (indicated by the larger shaded area in Figure 4B) than the *cis* flagellum, and the cell turns toward the light. As the cell rotates, the eyespot becomes shaded and the *cis* flagellum has the larger amplitude to reinforce the turning toward the light [22, 23]. This process results in the continuous turning of the cell toward the light. The response of the *trans* flagellum to a light signal has been referred to as flagellar dominance. Analysis of wild-type and *agg1* strains by high-speed cinematography shows that the flagellar dominance is reversed in the *agg1* strain. In *agg1*, the *cis* flagellum has the larger amplitude when lit, and the *trans* flagellum has the larger amplitude when shaded. Because the process is symmetrically reversed, the *agg1* cells respond to light by swimming away from it [24]. We suggest that *Agg1p*, *Agg2p*, and *Agg3p* block transmission of the light signal in the *cis* flagellum and reinforce the signal in the *trans* flagellum. When these proteins are reduced, the *cis* flagellum responds as the dominant flagellum.

It is interesting to note that *AGG2* and *AGG3* both have paralogs (Figures S1 and S2). Two of the three *AGG3* paralogs (DQ408775 and FAP 191) as well as *AGG3* were found by mass spectroscopy of flagella and were enriched in the membrane-matrix fraction [25]. The fourth paralog (155892) has not been shown to be a flagellar protein. Both the *AGG2* and *AGG3* paralogs are likely to have arisen by a recent duplication because they are tightly linked, respectively. It is interesting to speculate that different pairs of paralogs may be found in the *cis* and *trans* flagella to help to impart different responses to the light signal.

#### Supplemental Data

Supplemental Experimental Procedures and two figures are available with this article online at <http://www.current-biology.com/cgi/content/full/16/11/1147/DC1/>.

#### Acknowledgments

We thank J. Salisbury (Mayo Clinic, Rochester, MN) for the gift of the monoclonal antibody to centrin and Scott Henderson for performing transmission electron microscopy. We are also grateful to Naomi Morrissette, Jessica Esparza, and Jennifer Heeley for critical reading of the manuscript and many helpful discussions. This work was supported by grant GM-44467 to G.P. and GM-32843 to S.K.D. from the National Institutes of Health. We are deeply grateful to Elizabeth Harris for helping to track the history of the strain 622E used in the phototaxis analysis [24].

Received: January 19, 2006  
Revised: April 11, 2006  
Accepted: April 12, 2006  
Published: June 5, 2006

#### References

1. Foster, K.W., Saranak, J., Patel, N., Zarilli, G., Okabe, M., Kline, T., and Nakanishi, K. (1984). A rhodopsin is the functional photoreceptor for phototaxis in the unicellular eukaryote *Chlamydomonas*. *Nature* 311, 756–759.
2. Wilson, P.D. (2004). Polycystic kidney disease: New understanding in the pathogenesis. *Int. J. Biochem. Cell Biol.* 36, 1868–1873.
3. Pan, J., and Snell, W.J. (2000). Signal transduction during fertilization in the unicellular green alga, *Chlamydomonas*. *Curr. Opin. Microbiol.* 3, 596–602.
4. Simons, K., and Toomre, D. (2000). Lipid rafts and signal transduction. *Nat. Rev. Mol. Cell Biol.* 1, 31–39.
5. Bagnat, M., Keranen, S., Shevchenko, A., and Simons, K. (2000). Lipid rafts function in biosynthetic delivery of proteins to the cell surface in yeast. *Proc. Natl. Acad. Sci. USA* 97, 3254–3259.
6. Smyth, R.D., and Ebersold, W.T. (1985). Genetic investigation of a negatively phototactic strain of *Chlamydomonas reinhardtii*. *Genet. Res.* 46, 133–148.
7. Deane, J.A., Cole, D.G., Seeley, E.S., Diener, D.R., and Rosenbaum, J.L. (2001). Localization of intraflagellar transport protein IFT52 identifies basal body transitional fibers as the docking site for IFT particles. *Curr. Biol.* 11, 1586–1590.
8. Iomini, C., Tejada, K., Mo, W., Vaananen, H., and Piperno, G. (2004). Primary cilia of human endothelial cells disassemble under laminar shear stress. *J. Cell Biol.* 164, 811–817.
9. Kahn-Kirby, A.H., and Bargmann, C.I. (2005). TRP Channels in *C. elegans*. *Annu. Rev. Physiol.* 68, 719–736.
10. Corbit, K.C., Aanstad, P., Singla, V., Norman, A.R., Stainier, D.Y., and Reiter, J.F. (2005). Vertebrate Smoothened functions at the primary cilium. *Nature* 437, 1018–1021.
11. Teilmann, S.C., Byskov, A.G., Pedersen, P.A., Wheatley, D.N., Pazour, G.J., and Christensen, S.T. (2005). Localization of transient receptor potential ion channels in primary and motile cilia of the female murine reproductive organs. *Mol. Reprod. Dev.* 71, 444–452.
12. Watnick, T.J., Jin, Y., Matunis, E., Kernan, M.J., and Montell, C. (2003). A flagellar polycystin-2 homolog required for male fertility in *Drosophila*. *Curr. Biol.* 13, 2179–2184.
13. Trevino, C.L., Serrano, C.J., Beltran, C., Felix, R., and Darszon, A. (2001). Identification of mouse *trp* homologs and lipid rafts from spermatogenic cells and sperm. *FEBS Lett.* 509, 119–125.
14. Schermer, B., Hopker, K., Omran, H., Ghenoii, C., Fliegau, M., Fekete, A., Horvath, J., Kottgen, M., Hackl, M., Zschiedrich, S., et al. (2005). Phosphorylation by casein kinase 2 induces PACS-1 binding of nephrocystin and targeting to cilia. *EMBO J.* 24, 4415–4424.
15. Mahjoub, M.R., Qasim Rasi, M., and Quarmby, L.M. (2004). A NIMA-related kinase, *Fa2p*, localizes to a novel site in the proximal cilia of *Chlamydomonas* and mouse kidney cells. *Mol. Biol. Cell* 15, 5172–5186.
16. Mahjoub, M.R., Trapp, M.L., and Quarmby, L.M. (2005). NIMA-related kinases defective in murine models of polycystic kidney diseases localize to primary cilia and centrosomes. *J. Am. Soc. Nephrol.* 16, 3485–3489.
17. Champier, L., Sibille, N., Bersch, B., Brutscher, B., Blackledge, M., and Coves, J. (2002). Reactivity, secondary structure, and molecular topology of the *Escherichia coli* sulfite reductase flavodoxin-like domain. *Biochemistry* 41, 3770–3780.
18. Rohr, J., Sarkar, N., Balenger, S., Jeong, B.R., and Cerutti, H. (2004). Tandem inverted repeat system for selection of effective transgenic RNAi strains in *Chlamydomonas*. *Plant J.* 40, 611–621.
19. Segal, R.A., Huang, B., Ramanis, Z., and Luck, D.J. (1984). Mutant strains of *Chlamydomonas reinhardtii* that move backwards only. *J. Cell Biol.* 98, 2026–2034.
20. Silflow, C.D., Kathir, P., and Lefebvre, P.A. (1995). Molecular mapping of genes for flagellar proteins in *Chlamydomonas*. *Methods Cell Biol.* 47, 525–530.
21. Kamiya, R., and Witman, G.B. (1984). Submicromolar levels of calcium control the balance of beating between the two flagella in demembrated models of *Chlamydomonas*. *J. Cell Biol.* 98, 97–107.

22. Ruffer, U., and Nultsch, W. (1991). Flagellar photoresponses of *Chlamydomonas* cells held on micropipettes: II. Change in flagellar beat pattern. *Cell Motil. Cytoskeleton* **18**, 269–278.
23. King, S.J., and Dutcher, S.K. (1997). Phosphoregulation of an inner dynein arm complex in *Chlamydomonas reinhardtii* is altered in phototactic mutant strains. *J. Cell Biol.* **136**, 177–191.
24. Ruffer, U., and Nultsch, W. (1998). Flagellar coordination in *Chlamydomonas* cells held on micropipettes. *Cell Motil. Cytoskeleton* **41**, 297–307.
25. Pazour, G.J., Agrin, N., Leszyk, J., and Witman, G.B. (2005). Proteomic analysis of a eukaryotic cilium. *J. Cell Biol.* **170**, 103–113.
26. Luck, D., Piperno, G., Ramanis, Z., and Huang, B. (1977). Flagellar mutants of *Chlamydomonas*: Studies of radial spoke-defective strains by dikaryon and revertant analysis. *Proc. Natl. Acad. Sci. USA* **74**, 3456–3460.
27. Wang, Q., and Snell, W.J. (2003). Flagellar adhesion between mating type plus and mating type minus gametes activates a flagellar protein-tyrosine kinase during fertilization in *Chlamydomonas*. *J. Biol. Chem.* **278**, 32936–32942.

#### Accession Numbers

Three genes reported in this paper, *AGG2* (accession number [DQ065848](#)), *AGG3* ([DQ408775](#)), and *AGG4* ([DQ408776](#)), have been deposited in GenBank.